Effect of halides in the electrowinning of zinc. II. Corrosion of lead-silver anodes

M. Nicol, C. Akilan, V. Tjandrawan, J.A. Gonzalez

PII: S0304-386X(17)30381-X
DOI: doi: 10.1016/j.hydromet.2017.08.017
Reference: HYDROM 4639

To appear in: *Hydrometallurgy*

Received date: 4 May 2017
Revised date: 11 July 2017
Accepted date: 18 August 2017

Please cite this article as: M. Nicol, C. Akilan, V. Tjandrawan, J.A. Gonzalez , Effect of halides in the electrowinning of zinc. II. Corrosion of lead-silver anodes, *Hydrometallurgy* (2017), doi: 10.1016/j.hydromet.2017.08.017

Effect of Halides in the Electrowinning of Zinc.

II. Corrosion of Lead-Silver Anodes

M. Nicol[*1], C. Akilan[1], V. Tjandrawan[1] and J.A. Gonzalez[2]

1. School of Information Technology and Engineering, Murdoch University, Perth, WA 6150

2. Teck Metals Ltd., Applied Research and Technology, Trail, BC, Canada

Abstract

This paper summarizes experimental results obtained from a series of laboratory scale electrowinning tests conducted over 5 months to quantify the effects of halides (chloride, fluoride and bromide) on the performance and corrosion of lead-silver anodes under conditions similar to those used during the electrowinning of zinc. The parameters investigated include operating anode potential, corrosion rate and anode scale/cell mud generation rates. Information was also obtained on the consumption of halides and manganese ions and the composition of the anode scale and cell mud.

The results have confirmed plant observations of excessive anode corrosion and chlorine emissions at a chloride concentration of 400 mg/L but not at a concentration of 200 mg/L. It has also confirmed the importance of maintaining a suitable manganese(II) concentration in the electrolyte. Bromide and fluoride ions, albeit at lower concentrations, do not have measurable effects on anode corrosion.

Although a definitive explanation for enhanced local corrosion at high chloride concentrations has not been advanced, the nature of the accelerated corrosion suggests that a crevice-like corrosion process is responsible for localized massive corrosion. This has been attributed to the presence of high acidity and permanganate ions between the manganese oxide layer and the alloy surface.

Keywords: Zinc; electrowinning; anodes; corrosion; chloride

1 Introduction

In a previous paper (Nicol et al, 2017), the kinetics of the anodic oxidation of chloride ions on lead-silver anodes typical of those used in the electrowinning of zinc was reported. The literature on the oxidation of chloride ions and the effects of chloride on anode corrosion was also reviewed in this paper. A relevant literature review (Ivanov et al, 2000) describes the corrosion aspects of lead alloy anodes under electrowinning conditions. This paper summarizes experimental results obtained from a series of laboratory scale electrowinning tests conducted over 5 months to quantify the effects of halides (chloride, fluoride and bromide) on the performance of lead-silver anodes under conditions similar to those used during the electrowinning of zinc. The parameters investigated include operating anode potential, corrosion rate and anode scale/cell mud generation rates. Information was also obtained on the consumption of halides and manganese ions and the composition of the anode scale and cell mud.

2 Experimental details

2.1 Anodes

Rolled 6 mm Pb-0.5%Ag sandblasted 'T'–shaped anodes supplied by Teck Metals Ltd. were used as received. Average immersed anode dimensions were 80 mm x 40 mm. Initial electrode mass was about 390 g.

2.2 Electrolyte composition

All tests were conducted in an electrolyte containing 165 g/L H_2SO_4, 3 g/L Mn and various concentrations of halides (chloride, fluoride and bromide) as shown in Table 1. These concentrations were selected as being typical of those that could be expected in zinc electrowinning electrolytes, except for bromide that is normally not present in zinc electrolytes. AR grade 98% sulphuric acid, 32% hydrochloric acid, 48% hydrobromic acid, sodium fluoride (99% BDH), LH grade manganese metal flakes (dissolved in sulfuric acid) and high purity water (MilliQ-Millipore) were used to prepare electrolytes used in the study. Zinc sulfate was not added to the electrolyte to simplify the system by eliminating the cathodic deposition of zinc and thus not having to periodically harvest zinc sheets from the cathodes and replenish zinc in the electrolyte. This deviation from plant practice is considered

acceptable given that the anodic processes are unlikely to be affected by the cathodic reactions.

Table 1. Concentrations of halide ions (mg/L) in test solutions

Test No	1	2	3	4	5	6	7	8	9	10	11
Chloride	0	200	400	200	400	200	400	200	400	600	600
Fluoride	0	10	10	10	10	40	40	40	40	0	0
Bromide	0	0	0	10	10	0	0	10	10	0	0

Each test shown in Table 1 was duplicated and duplicates are referred to as (a) and (b).

2.3 Experimental set up

The corrosion tests were conducted in cylindrical cells consisting of 106 mm diameter polyethylene beakers with an electrolyte depth of 105 mm providing an effective solution volume of 900 mL. Each cell contained a single central anode with two 'T'–shaped facing Pb sheet cathodes (1 mm thick) that fitted through slots in a polypropylene lid. The dimensions of the cathodes (immersed dimensions 60 mm by 25 mm) were chosen to provide as uniform a current density as possible on each anode face. All tests were run in duplicate and a total of 18 cells were operated in three different water baths (1A-3B; 4A-6B; 7A-9B). Cell temperature was maintained at 40±1 °C. The cells were located under exhaust vents as shown in Fig. 1 for one set of 6 cells. The cells in each bath were connected electrically in series and a constant current power supply was used to provide an anodic current density of 480 A/m^2 (equivalent to a current of 3.25 A per anode).

2.4 Chemical analysis of electrolytes

The electrolytes were analysed every second or third day for acid, Mn(II), Cl^-, Br-, F- and Mn(III) ions throughout the test program and the concentrations of these elements (excluding Mn(III) that was not controlled) were maintained by addition of the relevant stock solutions. Solution volume was maintained by adding distilled water to compensate for evaporation losses. Acidity was monitored by titration with standard NaOH solution. Mn(II) ions were analysed by titration with standard EDTA solution. Chloride ions were analysed by potentiometric titration with standard silver nitrate solutions. Bromide and fluoride ions were analysed using the relevant ion selective electrodes. Mn(III) concentration was determined

by addition of excess Fe(II) ions followed by back titration of excess Fe(II) with standard potassium dichromate solution.

Fig. 1. Experimental set up for one of three modules

2.5 Measurement of potentials

Anode potentials (potential difference between the anode and a reference electrode) were measured three times per week using a mercury/mercurous sulphate reference electrode (MSE) with saturated potassium sulphate filling solution. The recorded potentials were converted to values versus standard hydrogen electrode (SHE) using a potential of 0.645 V versus SHE. A salt bridge (Luggin capillary) containing saturated K_2SO_4 was used. Anode potentials were measured by placing the Luggin capillary close to the centre of each side of the anodes and were not compensated for ohmic drop between the reference electrode and the anode surface.

Solution redox potential (ORP) was measured three times a week. The ORP probe had a gold electrode whose potential was monitored versus that of a MSE. Platinum electrodes could not be used because the solutions were saturated with hydrogen gas from the cathodes and the potential measured is lower than the equilibrium potential of the Mn(II)/Mn(III) couple as it

is a mixed potential comprising the dominant Mn(II)/Mn(III) and H^+/H_2 couples due to the high exchange current density for hydrogen evolution on platinum (but not on gold).

Current in each cell was monitored by measuring the voltage drop across a precision 0.1-ohm resistor connected in series with each cathode. Cell voltage was measured manually several times a week and cell current was logged every 5 minutes using a data acquisition system controlled by LabVIEW™.

2.6 Determination of corrosion rates

The anodes in each cell were removed each month for cleaning that involved brushing and collection of the loosely adhering scale. At the end each set of experiments, the mud in the bottom of the cells ("cell mud") and that adhering to the anode ("anode scale") was collected, washed, dried, weighed and analysed for Mn and Pb by X-Ray Fluorescence.

Also, at the conclusion of each test, after manual scraping of the loose scale from each anode, adherent oxides were removed by dissolution in a basic mannitol solution (20 g/L mannitol and 100 g/L NaOH). After the oxide layer was dissolved, anodes were rinsed with deionised water and left to dry in the air. The corrosion rates of the anodes was then determined from anode weight loss measurements and reported as total g Pb per total kAh passed at the specified current density.

3 Results and discussion

3.1 Corrosion tests at various halide concentrations

A total of 18 initial tests were conducted to evaluate the effects of chloride, fluoride and bromide ions on the corrosion rates of the Pb-Ag anodes. The test conditions and mass loss data are reported in Table 2 and Fig. 2. The service life of some anodes was limited because of severe corrosion localized mostly at the solution line that at times resulted in loss of the lower part of the anode as shown in some photographs in the Appendix. In these cases, the mass loss is not necessarily the same as the corrosion rate. For this reason, we use the term mass loss recognizing that for anodes 1,2,4,6 and 8, it is also the corrosion rate.

Table 2. Effect of halide ions on mass loss at a nominal Mn(II) concentration of 3 g/L

Cell	Cl-	F-	Br-	Anode life	Anode mass loss	Total mud generation rate	Cell mud generation rate
	mg/L	mg/L	mg/L	days	g/kAh	g/kAh	g/kAh
1A	-	-	-	150	0.91	3.42	3.59
1B	-	-	-	129	0.97	3.76	3.33
2A	200	10	-	150	1.54	4.66	4.07
2B	200	10	-	129	1.35	4.86	3.04
3A	400	10	-	78	35.83	4.81	45.04
3B	400	10	-	71	39.07	6.39	56.80
4A	200	10	10	143	1.65	4.99	2.89
4B	200	10	10	123	0.95	3.16	2.80
5A	400	10	10	74	38.18	5.94	42.82
5B	400	10	10	55	54.59	2.03	76.63
6A	200	40	-	143	1.35	5.33	3.18
6B	200	40	-	123	1.28	4.30	2.79
7A	400	40	-	103	8.07	3.91	14.92
7B	400	40	-	69	34.97	4.82	50.63
8A	200	40	10	120	1.58	4.12	3.96
8B	200	40	10	149	2.72	4.19	6.64
9A	400	40	10	72	25.12	3.32	41.59
9B	400	40	10	85	18.52	2.10	32.55

The results from duplicate experiments are generally satisfactory except for Run 7A for which the extent of mass loss appears to be lower than expected. However, in this case, the residue of the anode in the cell obtained from the dislodged part of the anode due to solution line corrosion was included in the residual anode mass and not in the cell mud component. Comparison with anode 7B gives an indication of the difference between mass loss and corrosion rate. In all cases in which the chloride concentration was nominally 400 mg/L, the mass loss was significantly greater than that obtained at the lower chloride concentration.

Published data on corrosion in the absence of chloride ions has been summarized (Newnham, 1992) and the rates vary between 1.1 and 3.8 g/kAh under similar conditions. In another study (McGinnity and Nicol, 2008), the corrosion rate of a similar PbAg (0.5% wt Ag) anode was measured over a period of 8 weeks in 170 g/L acid in the absence of chloride ions at 40^{o}C and 500A/m$^{2.}$ The corrosion rate obtained in the chloride-free electrolyte of 3.91 g/kAh was 3.3 times higher than that of the same alloy (1.20 g/kAh) in the same electrolyte containing 5 g/L manganese. The latter rate is comparable to corrosion rates obtained at

lower chloride concentration in Table 2 and indicates the importance of the formation of manganese oxides on the anode to reduce corrosion even in the absence of chloride

Additional information on the average chloride and manganese concentrations during each run is given in Table 3. Nominal target manganese concentration in all the tests was 3 g/L.

Table 3. Effect of halide and manganese(II) concentrations on anode mass loss and mud formation

Cell	Nom [Cl^-]	Mean [Cl^-]	Mean [Mn(II)]	Mean Mn/Cl	Anode mass loss	Total mud generation rate	Cell mud generation rate
	mg/L	mg/L	g/L		g/kAh	g/kAh	g/kAh
1A	-	-	2.22	-	0.91	3.42	3.59
1B	-	-	2.25	-	0.97	3.76	3.33
2A	200	182	2.19	12.0	1.54	4.66	4.07
2B	200	184	2.22	12.1	1.35	4.86	3.04
3A	400	237	1.54	6.5	35.83	4.81	45.04
3B	400	213	1.46	6.9	39.07	6.39	56.80
4A	200	183	2.32	12.7	1.65	4.99	2.89
4B	200	188	2.44	13.0	0.95	3.16	2.80
5A	400	271	2.26	8.3	38.18	5.94	42.82
5B	400	222	1.50	6.8	54.59	2.03	76.63
6A	200	180	2.28	12.7	1.35	5.33	3.18
6B	200	185	2.35	12.7	1.28	4.30	2.79
7A	400	330	2.16	6.5	8.07	3.91	14.92
7B	400	259	1.66	6.4	34.97	4.82	50.63
8A	200	183	2.29	12.5	1.58	4.12	3.96
8B	200	176	2.20	12.5	2.72	4.19	6.64
9A	400	262	1.77	6.8	25.12	3.32	41.59
9B	400	295	1.95	6.6	18.52	2.10	32.55

These results show that mean concentrations of chloride and manganese in the electrolyte were both lower than their nominal, target values. This is due to the fact that chemical analyses were conducted only two or three times per week and concentrations were only adjusted to the target values after analysis. Consumption of manganese and chloride during periods between analyses resulted in lower average values in the bulk electrolyte than those targeted. Also, proportionally, the decreases in manganese concentration were greater than those of chloride. From the average concentrations, average total Mn/Cl ratios were calculated and are shown in Table 2. The Mn/Cl ratio is lower for anodes that were subject to severe corrosion, indicating very large decreases in manganese during those tests together

with large chloride losses. In general, at 200 mg/L Cl, high Mn/Cl ratios (between 12 and 13) resulted in the lowest anode corrosion rates. Additional tests should be carried out to investigate whether operation at high Mn/Cl ratios (close to 12) are also effective to offset the impact of high chloride (400 mg/L) concentrations in the electrolyte.

Selected photos of some of the corroded anodes are given in the Appendix. Examination of the photographs reveals that those anodes that operated with 400 mg/L chloride all showed massive corrosion predominantly at the solution line although Cell 9 anodes revealed other localized areas of corrosion. There is also evidence of incipient localized corrosion in the anodes from Cells 4A and 8B both of which had 200 mg/L chloride. Even anodes from cells 10B and 11A (Section 4) that only operated for 44 d showed evidence of localized corrosion in the presence of 600 mg/L chloride.

3.2 Effect of chloride concentration on anode corrosion

Results show (Table 3, Figure 2) that the highest anode mass losses were observed in those tests (cells 3, 5, 7 and 9) carried out at the higher chloride concentration (400 mg/L). In these tests, anodes had short service lives (between 55 and 103 d) given their catastrophic failure. While chloride concentration has a significant impact on anode corrosion rate, it appears that fluoride and bromide ions do not have an impact on the anode corrosion rate.

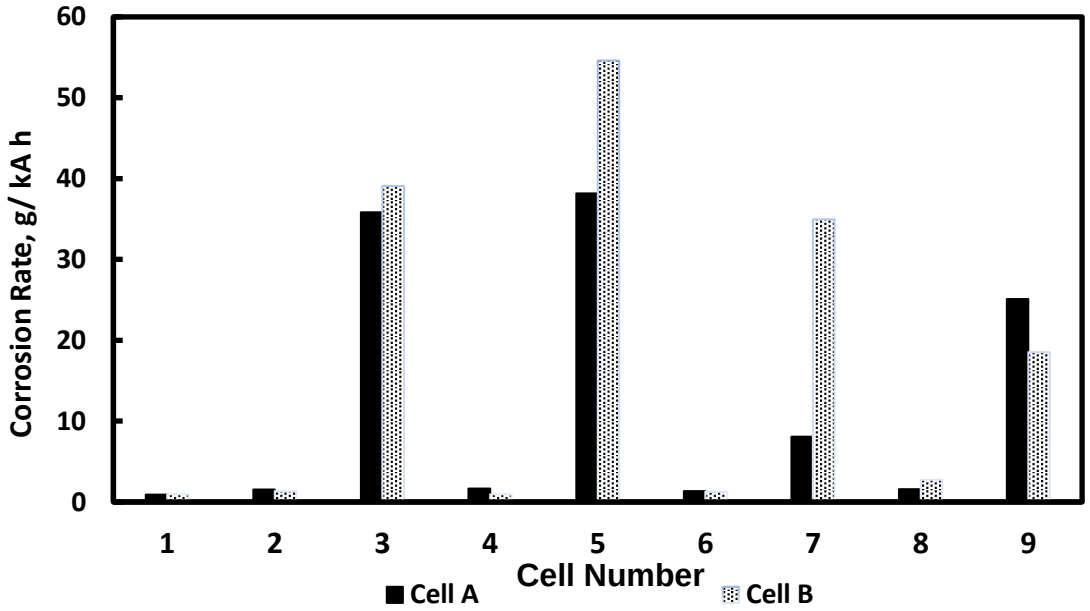

Fig. 2. Mean rates of anode mass loss. 200 mg/L chloride in cells 2,4,6 and 8. 400 mg/L chloride in cells 3,5,7,9.

Although there does not seem to be a clear impact of bromide ions on the anode corrosion rates (compare the rates for runs 2 and 4 and runs 6 and 8), it should be noted that about 60 to 90% of the bromide added was consumed each day as bromide was readily oxidized to bromine. On the other hand, as expected, the fluoride ion concentrations were almost constant throughout each experiment. Bromide oxidation is expected given the relatively low standard thermodynamic potential of the bromine/bromide couple of 1.07V versus that of oxygen evolution (1.23 V) which also has a relatively high overpotential (~ 0.6 V) in this system. The high thermodynamic potential of the fluorine/fluoride couple of 2.92V precludes oxidation of fluoride.

The average mass loss data for all anodes operated at two different chloride concentrations are summarized in Table 4.

Table 4. Mean rates of mass loss

[Cl] mg/L	Mean mass loss, g/kAh
0	**0.94**
200	**1.55**
400	**31.8**

It is evident that the average corrosion rate at 200 mg/L Cl is almost 60% higher than that in the absence of chloride ions. However, the rate of mass loss is up to twenty times higher at 400 mg/L Cl than at 200 mg/L. It is not known if higher concentrations of manganese than those tested here would have prevented this high corrosion rate, but consumption of manganese was very significant indicating that formation of MnO_2 was greater in the presence of high levels of chloride but this was not sufficient to offset the corrosion in the presence of chloride (particularly at the solution line where it was most severe).

3.3 Correlation of corrosion rate with manganese and chloride ion consumption

Results summarized in Figure 3 show that the manganese consumption (or manganese addition required during the tests) for all anodes operated with a target 200 mg/L Cl concentration was approximately the same at about 4g Mn/kAh. Assuming that consumption of manganese is primarily due to oxidation to MnO_2 by the reaction

$$Mn^{+2} + 2H_2O = MnO_2 + 4H^+ + 4e \quad (1)$$

an average current efficiency for this reaction at 200 mg/L chloride can be calculated as 0.8%.

However, for those anodes that strongly corroded (cells 3,5,7,9 containing 400 mg/L chloride) the consumption of manganese was initially about the same but increased substantially at some rather arbitrary point in the life of these anodes. This suggests that additional Mn-consuming reactions were triggered by the presence of higher concentrations of chloride in the electrolyte.

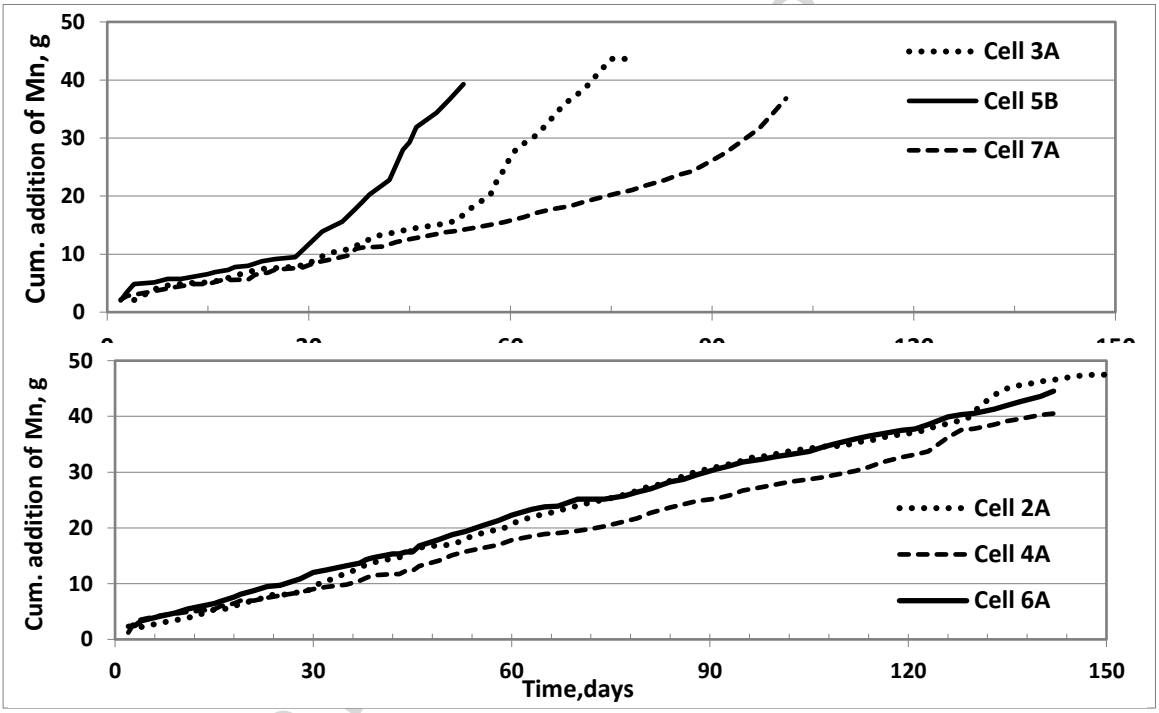

Fig. 3. Cumulative addition of manganese to selected cells. Lower plot for cells with 200 mg/L chloride and upper for 400 mg/L chloride.

Data for the consumption of chloride is summarized in Fig. 4. Similar trends to that of the manganese consumption are observed with the exception that:

a) Rates of consumption (on a molar basis) of chloride (0.0028 mol/kAh) are up to 25 times lower than that of manganese (0.07 mol/kAh)
b) The rate of consumption of chloride is much greater for cells operated with nominally 400 mg/L Cl than those at 200 mg/L Cl .

The chloride consumption rate obtained in this study can be compared with the value of 0.07 mol/kAh obtained in a previous study (Nicol et al, 2017) conducted for only 5 h using similar anodes but an electrolyte containing nominally 600 mg/L Cl and 2.5 g/L Mn. This large difference in chloride consumption rate for short tests versus that measured in longer tests can be attributed to the fact that until the manganese oxide layer has sufficiently grown on the anode surface, the rate of oxidation of chloride can be very high. This is apparent (Fig. 4) in the rapid increase in chloride consumption shown in the initial 3-5 h of oxidation of the anodes and is routinely seen in the industry where chlorine evolution is largest for the first few hours of electrolysis when new anodes are initially placed in electrowinning cells.

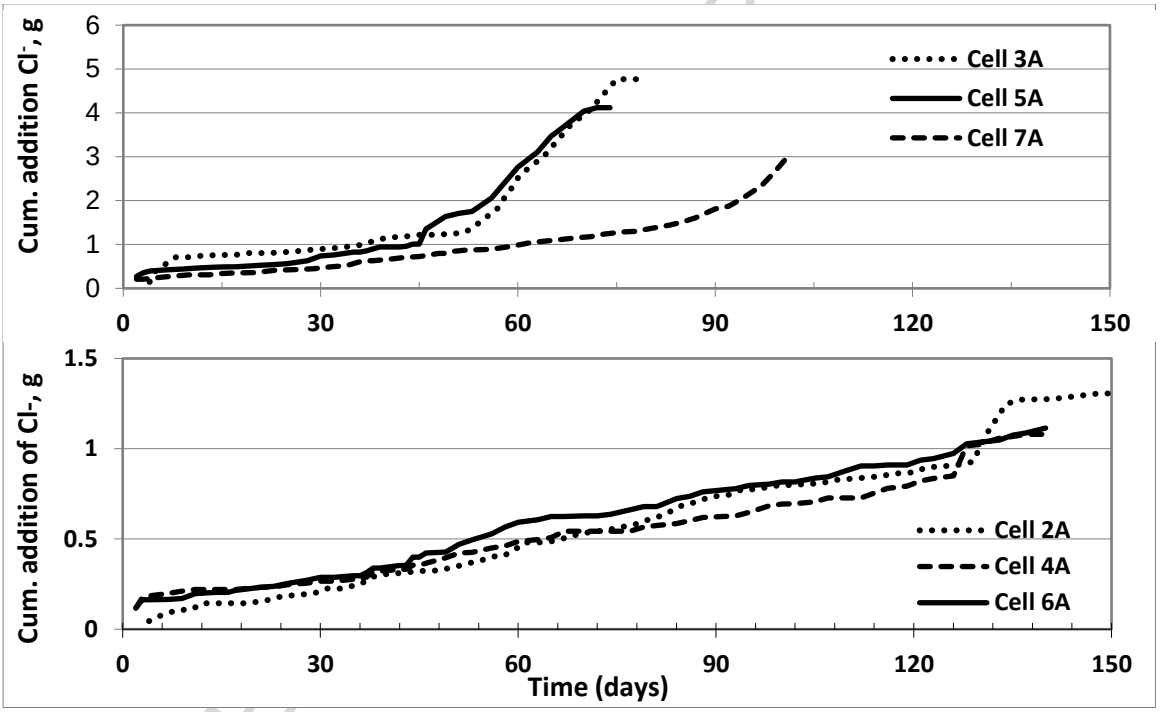

Fig. 4. Cumulative addition of chloride to selected cells. Lower plot for cells with 200 mg/L chloride

It is interesting to note that, in other unpublished work in a local copper EW pilot plant, the rate of chloride consumption on lead-calcium-tin anodes under typical copper electrowinning conditions was found to be 0.03 mol/kAh at a current density of 300 A/m^2 in an electrolyte containing 25 mg/L Cl and no manganese. This significant oxidation of chloride at low chloride concentrations in absence of manganese ions highlights the significant effect that manganese oxides can have on reducing the rate of chloride oxidation.

A plot of the average daily addition of manganese versus the mean mass loss (Figure 5) shows that there is a correlation between these parameters. Cell 5B which contained 400 mg/L Cl started to follow this pattern of increased consumption of manganese and chloride after about 30 days of operation (Appendix C; Figure C5), and the anode eventually failed after 55 d. Cell 8B that contained 200 mg/L Cl and exhibited a slightly higher corrosion rate also showed a slight increase in manganese consumption but only after about 105 d of operation.

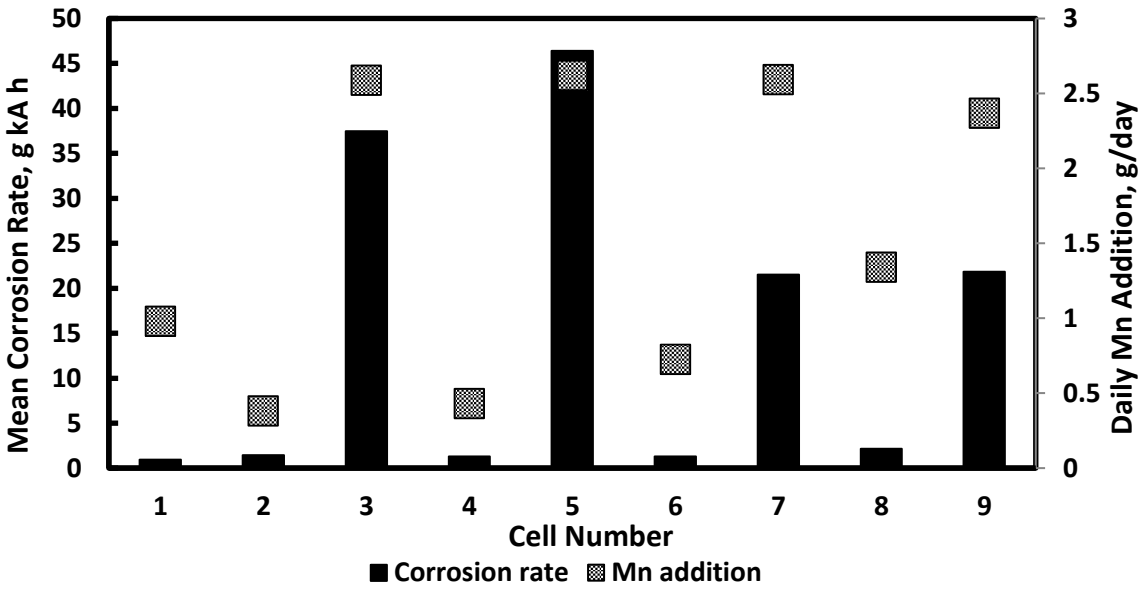

Fig. 5. Relationship between mean (cells A and B) mass loss and mean daily rate of manganese addition.

3.4 Cell mud generation

The rates of cell mud generation presented in Figure 6 were calculated from the total cell mud generated by each anode over the 150 d test period or over the life of each anode (if early failure was observed) and results for duplicate runs (A and B) were averaged and presented in this figure. These cell mud data include remnants of the non-corroded anode in the cell mud from loss of the lower parts of the anodes due to solution-line corrosion for cells operated at the higher chloride concentration.

Results shown in Table 6, show that anodes that operated at the higher chloride concentration (cells 3,5,7,9) consistently produced the greatest mass of cell mud and had the highest anode

corrosion rates. Higher mud production was also associated with higher manganese consumption (as shown in Fig 5).

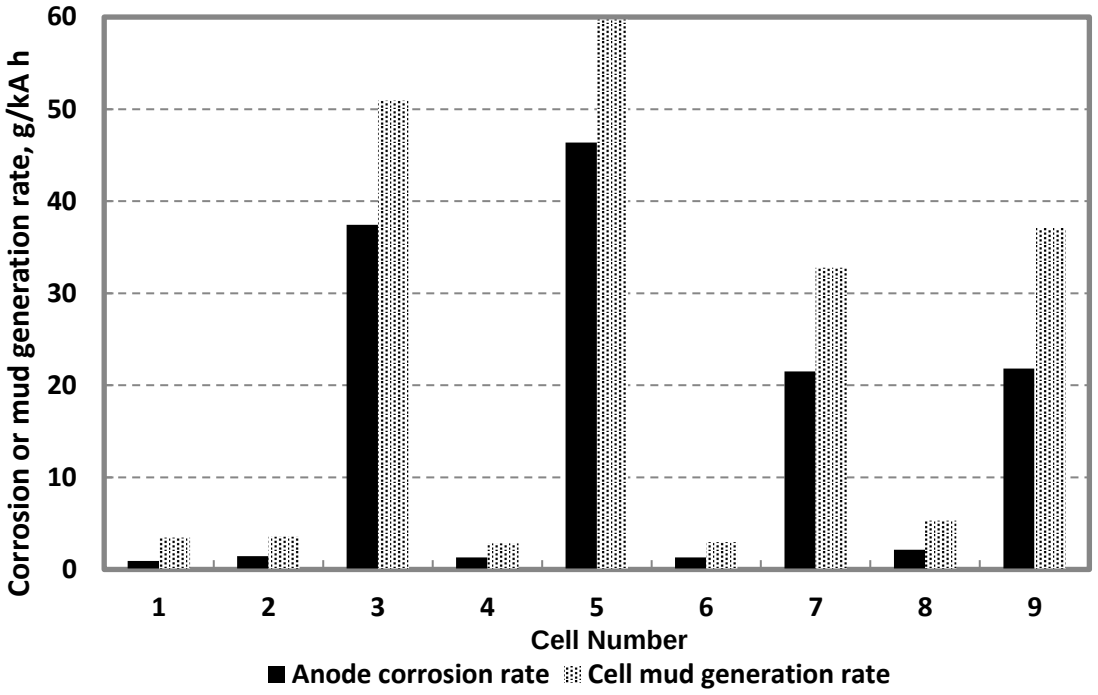

Fig. 6. Comparison of mass loss with cell mud generation rate.

3.5 XRF analysis of anode scale and cell mud

The manganese and lead content in the anode scale and in the cell mud obtained by XRF analysis are presented in Fig. 7 and Fig. 8. XRF results show that both anode scale and cell mud from cells 3, 5 and 7 contain a higher proportion of lead than of other elements. However, it should be mention that the mud from these cells contains not only cell mud but also corroded anode fragments that are inseparably mixed with cell mud.

Figure 7 shows that the percentage of manganese present in the anode scale was about 50% except for cells 3 & 5. This suggests that the major compound that precipitates in significant amounts on the lead anode, and becomes part of the surface layer, is MnO_2. This is also observed in practice. However, it should also be noted that cells 3 and 5 operated at a higher chloride concentration of 400 mg/L and had a shorter life span.

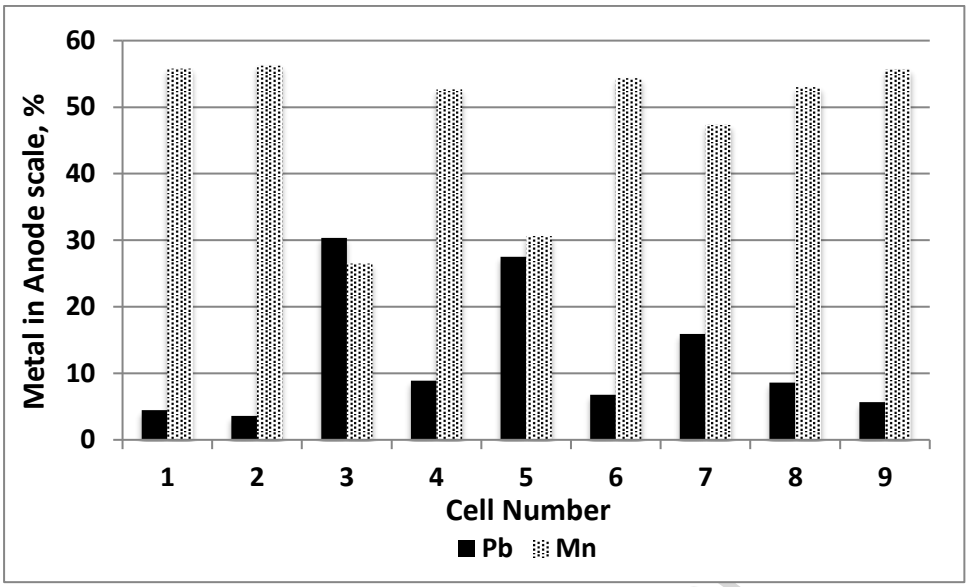

Fig. 7. Lead and manganese in the anode scale.

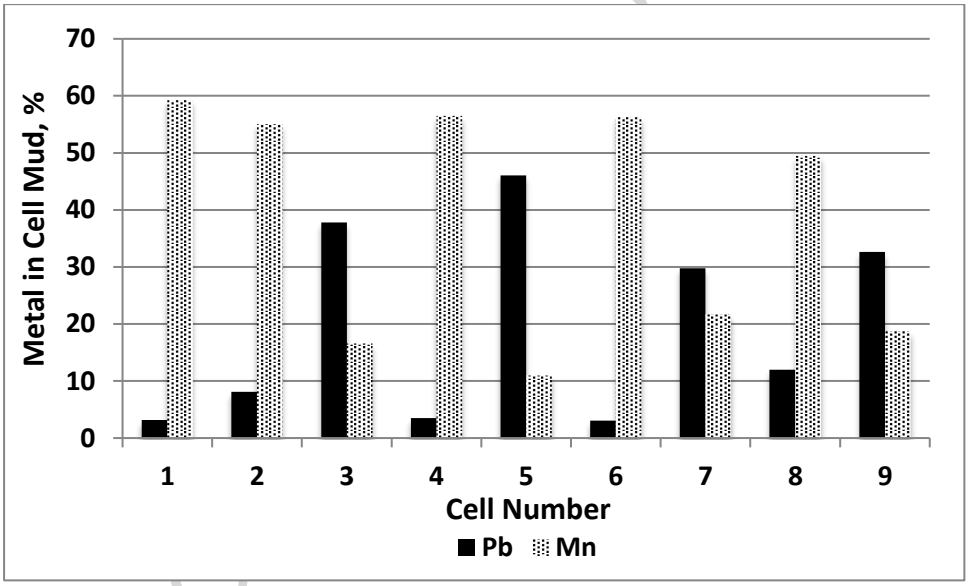

Fig. 8. Lead and manganese content in the cell mud

Further studies on selected cell mud and anode scale samples were carried out using X-ray diffraction which detected the presence of MnO_2 and PbO_2 and, in some cases, $PbSO_4$. In the mud from cell 1A which operated without chloride, XRD detected only MnO_2 while in mud from cell 7A (400 mg/L chloride) both MnO_2 and PbO_2 were found. This difference is possibly due to the fact that the mud in the case of cell 7A also contained a large fragment of corroded anode (Appendix).

3.6 Anode and solution potentials

Typical changes in the anode potentials during the operational period are shown for two cells in Fig. 9.

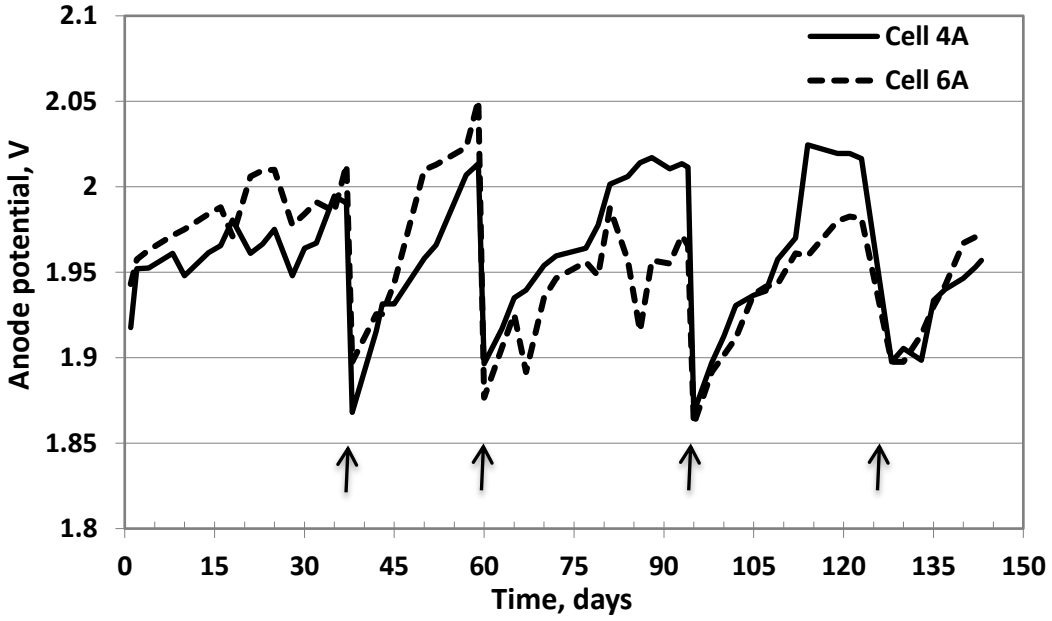

Fig. 9. Variation of anode potentials with time. Anodes were removed for cleaning at the times indicated.

As can be seen in Fig. 9, the anode potentials increase slowly with time. After anode mud removal and cleaning (approximately every 30 days), the potentials decrease by over 100 mV and then slowly increase until the next cleaning cycle. These drops are similar to those experienced in industrial cells, as indicated by cell voltages that decrease after anode cleaning or replacement of the anodes. Plant experience has also shown that the evolution of chlorine from a particular cell in a tankhouse increases after freshly cleaned (or new) anodes are returned to the electrolysis cells. Data in this regard was provided in Part 1 (Nicol et al, 2017). This increase in anode potential is due to the increasing impedance of the thickening manganese oxide layer on the anodes.

The average (from a and b replicates) anode potentials in each of the tested cells over their operating period for cells nominally 0, 200 mg/L Cl and 400 mg/L are are are summarized in Table 5. The anode potential at the higher chloride concentration is close to 40 mV lower than that at the lower chloride concentration. This difference could be expected given that the

presence of chloride ions reduces the potential for oxygen evolution as described in a previous paper. (Nicol et al, 2017)

Table 5. Average anode potentials at 480 A/m^2.

Cell	[Cl]	Average Potential
	mg/L	V
1	0	1.949
2	200	1.966
3	400	1.911
4	200	1.955
5	400	1.885
6	200	1.955
7	400	1.952
8	200	1.963
9	400	1.936
Average	200	1.960
Average	400	1.921

The oxidation reduction potential (ORP) versus SHE, of electrolytes tested measured using a gold/reference electrode for all the cells operated with 200 and 400 mg/L chloride are summarized in Fig. 10.

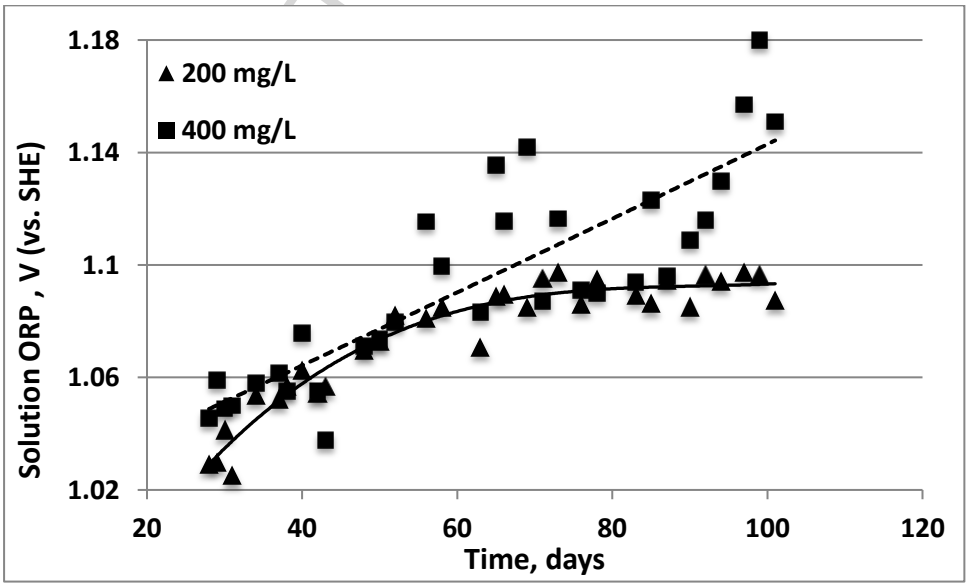

Fig. 10. Effect of chloride concentration on the increase in average solution potentials (ORP) with electrolysis time.

In this system, the solution potential is dominated by the Mn(III)/Mn(II) couple. Thus, the increasing solution potentials shown in Fig. 10 indicate that the Mn(III) concentration is slowly increasing with time. Using an estimated formal potential for the Mn(III)/Mn(II) couple under these conditions of 1.41 V and a total Mn ion concentration of 2.2 g/L, a Mn(III) concentration of 0.7 x 10^{-3} mol/L or 39 mg/L for a solution potential of 1.11V is calculated which is consistent with the assay data shown in Fig. 11.

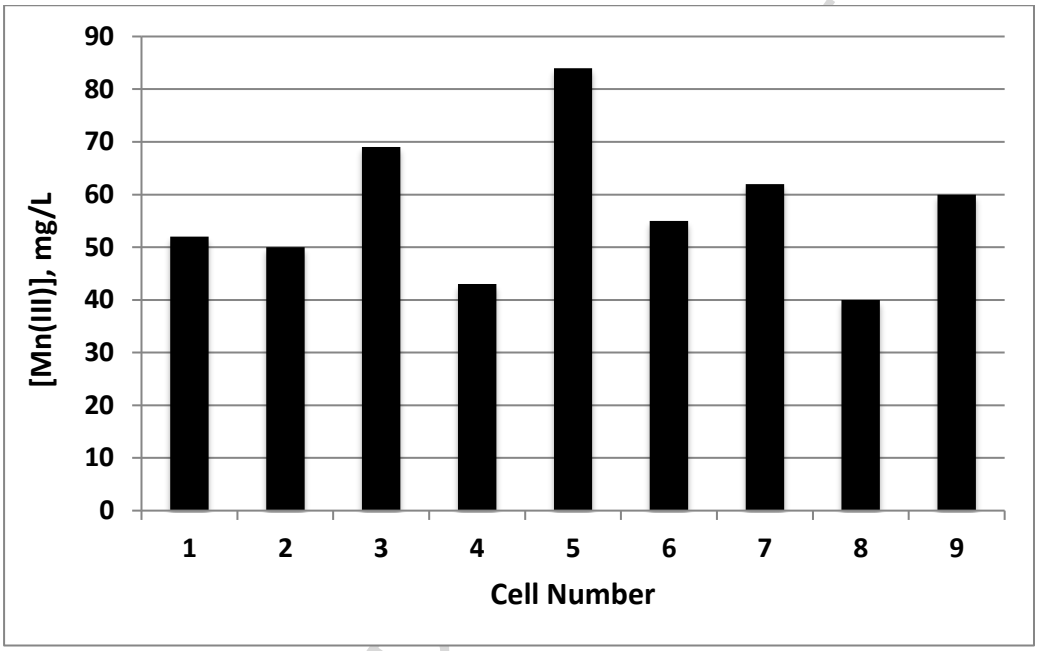

Fig. 11. Average Mn(III) concentrations in each cell over the first 90 days. Cells 3,5,7 and 9 had the higher chloride concentration.

The average Mn(III) concentration for cells operated with 200 mg/L chloride was 47 mg/L and was 69 mg/L for cells with 400 mg/L chloride. This difference suggests that increased rates of chloride oxidation to chlorine results in increased manganese(III) concentrations. The increased manganese(III) concentration will subsequently lead to greater production of MnO_2 via the disproportionation reaction (2) that then leads to enhanced formation of MnO_2 and increased cell mud formation

$$2Mn^{3+} + 2H_2O = MnO_2 + Mn^{2+} + 4H^+ \quad (2)$$

4. Control of manganese(III) concentration

An additional set of tests were carried out in order to investigate the effect of control of the manganese(III) concentration on the corrosion of Pb-Ag anodes. Hydrogen peroxide was continuously pumped into a cell to reduce the formed manganese(III) ions back to manganese(II) ions by the following reaction and thereby minimize formation of MnO_2 on the surface of the anodes (Gonzalez, 1998),

$$2Mn(III) + H_2O_2 + 2H^+ = 2Mn(II) + 2H_2O \qquad (3)$$

The tests were performed under accelerated corrosion conditions by adding 600 mg/L of chloride ions to the base electrolyte (165 g/L H_2SO_4 and 3 g/L Mn) in the absence and presence of hydrogen peroxide. Tests were run in duplicate. Four cells were operated for about 44 days under the conditions summarised in Table 6.

Table 6. Conditions for anode corrosion tests with and without peroxide

Cell	Pb-Ag Anode used	Current density A/m^2	Volume of solution mL	H_2O_2 flow rate mmol/h
10A	New sandblasted anode	466	900	-
10B	Used anode from previous Cell 1B	495	900	-
11A	Used anode from previous Cell 1A	480	1000	4.00
11B	New sandblasted anode	480	1000	2.57

The tests without peroxide addition (Cells 10A & 10B) were performed with the cells used in the previous tests (Figure 1) and one power supply was used to provide a current of about 3.4 A to each anode. The tests with peroxide addition (Cells 11A & 11B) were performed using 1 L glass beakers on temperature controlled hot plates so that changes in colour of the electrolyte due to the presence of manganese(III) ion could be closely monitored. Hydrogen peroxide was pumped regularly into the electrolyte using a peristaltic pump with a variable timer with the pumping time adjusted such that the pinkish colour due to manganese(III) just disappeared due to reaction with peroxide. Solution potential measurements were found to be unreliable as a means of control in the presence of peroxide, and colour change was the main indicator of the reduction of manganese(III).

The results of these tests are summarised in Table 7. The corrosion rate (in g lead/kAh) of the anodes operated in the absence of manganese(III) by means of the addition of hydrogen peroxide (Cells 11A & 11B) were lower than those operated without manganese(III) control (Cells 10A & 10B). The corrosion rate was found to be higher in cells 10B and 11A that operated with the used anodes. The corrosion rate measurements are subject to some error due to the very small mass loss over the limited period. Because of this, it is not known whether these anodes would be subject to accelerated corrosion at some point in their life such as that experienced by the anodes in the original set of tests with 400 mg/L chloride ions.

The cells operated with control of manganese(III) had less anode scale and no cell mud and, as a result of this, these cells consumed much less acid, manganese and chloride ions. This was expected given that oxidation of manganese ions was prevented by the addition of peroxide. The anode potentials for the cells with redox control were also lower compared to those without redox control.

Table 7. Summary of the results for the tests with and without peroxide addition

Cell		**10A**	**10B**	**11A**	**11B**
Anode potential start	V	1.90	1.88	1.86	1.95
Anode potential final	V	2.03	2.00	1.93	1.99
Solution Eh start	V	1.00	1.03		
Solution Eh final	V	1.12	1.12		
Total acid addition	g	36.1	35.9	25.8	15.6
Total Mn addition	g	13.9	18.2	1.7	2.1
Total Cl^- addition	g	1.21	2.50	0.68	0.65
$[Mn^{3+}]$ average	mg/L	66	68	0	0
Anode scale	g	18.9	16.4	6.2	2.8
Cell mud	g	8.2	24.4	0.00	0.00
Anode scale + cell mud	g	27.2	40.7	6.2	2.8
Anode weight loss	g	3.0	8.2	5.9	0.7
Anode operating period	hours	1054	1054	1060	1056
Corrosion rate	**g/kAh**	**0.84**	**2.27**	**2.03**	**0.22**
Anode scale generation rate	**g/kAh**	**5.24**	**4.53**	**2.13**	**0.88**
Cell mud generation rate	**g/kAh**	**2.28**	**6.75**	**0**	**0**

It is interesting to note that the consumption of chloride ions was lower in the cells operated with addition of peroxide that presumably can also act as a reductant for any produced chlorine. It is perhaps significant that the corrosion rate without peroxide in these tests appears to be noticeably lower than that shown in Table 3 for the original set of tests. This

could be because the manganese concentration was maintained daily during the tests shown in Table 7 while it was only adjusted twice or three times per week in the original tests. The decay in manganese concentration is such that the levels can fall to low values even after one day given the relatively large anode area to solution volume ratio. Thus, it is possible that the manganese ion concentration was too low to minimize corrosion by chloride ions for a significant fraction of the service life of the anodes in the original test work.

5 Proposed mechanism of accelerated corrosion at high concentrations of chloride ions

The many processes involving anode oxidation, oxygen evolution and the oxidation of other solution species such as iron(II), cobalt(II), manganese(II) and chloride ions that occur on the surface of lead alloy anodes during the electrowinning of base metals in sulphate solutions serve to create a system that is heterogeneously complex with porous layers of various lead species. The addition of manganese ions results in both additional anodic reactions and the formation of manganese oxides together with lead oxides. It is therefore not surprising that a generally accepted chemical description of this complex system has not yet been developed. The following is another contribution to the understanding of the interactions in this system. Several experimental observations made during this investigation and reported in the previous paper (Nicol et al, 2017) have a bearing on the nature of the interactions of chloride and manganese ions at the anodes during electrowinning of zinc. Some of the most important of these are

1. The rate of corrosion of the anodes is strongly dependent on the concentration of chloride ions with significantly enhanced rates at 400 mg/L relative to 200 mg/L.

2. The presence of manganese ions acts to reduce the deleterious effects of high chloride ion concentrations.

3. The rate of anodic oxidation of chloride ions **in the absence of manganese ions** is mass transport controlled at Pb-Ag anodes under typical zinc electrowinning conditions. (Nicol et al, 2017)

4. The rate of anodic oxidation of chloride ions is suppressed in the presence of manganese ions at concentrations above about 1 g/L. (Nicol et al, 2017)

5. In presence of hydrogen peroxide in amounts sufficient to reduce manganic ions and to minimize formation of a manganese scale on the anode, the rate of corrosion is reduced even in presence of 600 mg/L Cl. The consumption of chloride is also reduced in the absence of manganese(III) ions in the bulk electrolyte. (Nicol et al, 2017)

6. Accelerated corrosion appears to be initiated at some point in the life of the anode and this initiation time varies from anode to anode. The severe corrosion observed in failed anodes appears to be localized and often close to the solution line.

7. The rate of oxidation of chloride and manganese ions increases substantially at the point of accelerated corrosion.

8. Chlorine gas is evolved at Pb-Ag anodes operated at 440 Am^{-2} from solutions containing 300 mg/L Cl even in the presence of 4 g/L Mn albeit at a rate which is much smaller than in the absence of manganese ions. (Nicol et al, 2017)

9. The purple colour of permanganate is visible streaming from within the scale on the anodes when removing them from the cells.

10. In addition to the above, unpublished research also showed that accelerated local corrosion of Pb-Ag anodes can ocur even in absence of chloride ions. Thus, a rolled 0.6% Ag alloy was grit blasted and operated for 7 days in a solution of 170 g/L acid and 5 g/L manganese at 530 A/m^2. Fig. 12 is an example of such corrosion near the top of the anode from which the anode scale had been removed.

Fig. 12. Corrosion of a Pb-Ag anode close to the solution line

Other tests were carried out in in which the electrolyte occluded behind a thick MnO_2 scale on an anode operating under the above conditions was sampled with a syringe after 7 days and analysed by a combination of titration and UV-VIS spectrophotometry with the results shown in Table 8.

Table 8. Comparative analyses of various compounds in the bulk and in the electrolyte occluded behind the anode layer

Species	Occluded Electrolyte	Bulk Electrolyte
[Mn] total (g/L)	1.1	4.8-5.6
$[MnO_4^-]$ (gMn/L)	1.1-1.3	Not detected (UV-VIS)
$[Mn^{+3}]$ (g/L)	Not detected (UV-VIS)	0.005 to 0.0150
$[H_2SO_4]$ (g/L)	206	131

These results suggest that the Mn ions within the scale are predominantly present as permanganate with presumably, only small amounts of manganese(II). In needs to be

mention, that manganese(III) is difficult to detect spectrophotometrically in presence of permanganate and therefore could also be present in the occluded electrolyte. Furthermore, available evidence now suggests that the rates of the main anodic oxidation reactions (4) to (7) on the outer surface of the manganese scale are slow and that all the anodic reactions predominantly occur at the oxidised alloy surface beneath the scale.

$$2Cl^- = Cl_2 + 2e \quad (4)$$

$$2H_2O = O_2 + 4H^+ + 4e \quad (5)$$

$$Mn^{+2} = Mn^{3+} + e \quad (6)$$

$$Mn^{+2} + 4H_2O = MnO_4^- + 8H^+ + 5e \quad (7)$$

Note that in these equations, Mn(II) is written as Mn^{2+} and Mn(III) as Mn^{3+} although in sulphate solutions the predominant species are not the aquo-ions but sulphate and bisulfate complexes. (Kelsall et al, 2000)

Previous studies have demonstrated that oxygen evolution occurs beneath the manganese scale (McGinnity and Nicol, 2014) and this is supported by the high acid concentration measured in the occluded electrolyte.

Several mechanisms have been proposed in the limited literature on the interactions of manganese and chloride ions during the electrowinning of zinc, the most recent (Kellsal et al, 2000) of which is probably the most comprehensive from a theoretical point of view. On the question of corrosion the authors concluded that

a) “Manganese dioxide deposited on lead alloy anodes also decreases the chlorine evolution rate compared with bare anodes, the effective current efficiency for chlorine (evolution) on PbO_2 anodes covered with MnO_2 being low and oxygen evolution favoured, probably by MnO_2 forming a diffusional barrier to chloride ions”.

This conclusion is in accord with the results obtained in a previous publication (Nicol et al, 2017) in which it was observed that the anodic oxidation of chloride is inhibited in the presence of manganese ions. In a study of oxygen and chlorine evolution from manganese oxide-coated DSA anodes, it was shown (Bennett, 1980) that anodically produced “manganese dioxide” results in almost complete suppression of chlorine evolution as a result of a) a very low exchange current for chlorine evolution on the amorphous oxide layer and b)

the diffusion barrier provided by the oxide layer that prevents access of chloride ions to the underlying electrode surface.

b) "Any chlorine that does form is scavenged homogeneously by Mn(II) species."

The reaction that scavenges the chlorine is suggested as

$$Mn^{2+} + Cl_2 + 2H_2O = MnO_2 + 4H^+ + 2Cl^- \quad (8)$$

This reaction was also proposed as the reason for lower rates of chlorine evolution into the gas phase in the presence of manganese(II) ions (Hierzyk et al, 1969; Pakhomova and Marenkova, 1966) and for the lower amounts of chlorine in both the solution and gas phases in the presence of manganese(II) ions. Implicit in these suggestions is that accelerated rates of anode corrosion are due to anodically generated chlorine which chemically attacks the alloy. Details of such attack have not been studied and this remains an unproven albeit plausible hypothesis.

Although chlorine attack of the anode is possible, there is other evidence which suggests that the rate of above reaction (8) to produce MnO_2 is not significant. Thus, although the thermodynamics of this reaction are favourable, its kinetics do not appear to be rapid enough under typical electrowinning conditions. Thus, studies of the kinetics of the reaction between permanganate ions and chloride ions in acid solutions (Liu et al, 1996; Levanov et al, 2006) have shown that chlorine and manganese(III) ions are the products of reaction in presence of excess manganese(II) ions in acidic solutions and that the produced solutions are stable for long periods without precipitation of MnO_2. The alternative scavenging reaction

$$Mn^{2+} + 1/2Cl_2 = Mn^{3+} + Cl^- \quad (9)$$

has an equilibrium constant of 0.016 at 40^{o}C which is adequate for removal of chlorine only at low chloride and high manganese ion concentrations. In addition, although there have not been actual quantitative studies of the kinetics of this reaction, qualitative observations (Liu et al, 1996; Levanov et al, 2006; Ibers and Davidson, 1950) suggest that it is very slow in absence of catalysts.

Other reactions which need to be considered in light of the observation of permanganate behind or within the scale on the anodes are the reduction of permanganate by manganese(II) and also by chloride ions.

$$MnO_4^- + 4Cl^- + 8H^+ = Mn^{3+} + 4H_2O + 2Cl_2 \quad (10)$$

$$MnO_4^- + 4Mn^{2+} + 8H^+ = 5Mn^{3+} + 4H_2O \quad (11)$$

The stoichiometry and kinetics of these reactions in acidic perchlorate solutions have been published [Liu et al, 1996; Rosseinsky and Nicol, 1965). Both of these reactions are 1st-order in permanganate and 2nd-order in the reductant and the rate is therefore sensitive to the chloride or manganese(II) concentrations. In addition both reactions have a strong dependence on the acidity. Table 9 summarizes some calculations of the rates of these reactions in terms of the half-life ($t_{1/2}$) of permanganate under various conditions.

Table 9. Comparative kinetics of the reduction of permanganate by chloride and manganese(II) ions at 40°C

$[H^+]$ M	$[Cl^-]$ M	$[Cl^-]$ mg/L	$t_{1/2}$ min	[Mn(II)]] M	[Mn(II)]] g/L	$t_{1/2}$ min
1	0.01	355	1155.0	0.05	2.75	0.88
1.5	0.01	355	342.2	0.05	2.75	0.68
2	0.01	355	144.4	0.05	2.75	0.55
1	0.02	710	288.8	0.01	0.55	22.07
1.5	0.02	710	85.6	0.01	0.55	16.92
2	0.02	710	36.1	0.01	0.55	13.72

It is apparent that the rate of reduction by manganese(II) ions is faster than that by chloride ions but the rates are comparable at low manganese(II) ion concentrations and high chloride concentrations. Given the above rates of reduction of permanganate, and the observation of the presence permanganate in the electrolyte within the manganese scale suggests that the manganese(II) and chloride ion concentrations are low in the occluded electrolyte.

It was suggested that permanganate ions are in some way associated with accelerated corrosion of this type, which was similar to that observed above in the presence of chloride ions in that it tended to be initiated in particular spot or area on the anode, and was often observed at the solution line.

The observations of crevice-like corrosion in the absence of chloride ions (Fig. 12) suggested the possible role of permanganate in such corrosion. It is also possible that dissolved chlorine could play a similar role and, if so, the data in Table 9 are relevant. Thus, in the absence of manganese (II) ions close to the alloy surface, chlorine could be produced by the above reaction with electrogenerated permanganate ions and/or anodic oxidation at the alloy surface

(it has been shown in the previous paper that chloride is not oxidised on a MnO_2 surface) and accelerated corrosion would then occur. On the other hand, in the presence of sufficient concentrations of manganese(II) ions, permanganate would be reduced by manganese(II) in preference to reduction by chloride and neither permanganate nor chlorine would be present close to the alloy surface. This could explain the sensitivity of anode corrosion to both the manganese(II) and chloride ion concentrations and also to plant observations that the problem can be mitigated by maintaining a minimum manganese(II) concentration in the electrolyte. Another consideration involves the disproportionation of Mn(III) to form MnO_2 inside the anode scale i.e. the scale grows from the inside.

$$2Mn^{3+} + 2H_2O = Mn^{2+} + MnO_2 + 4H^+ \qquad (2)$$

The important observation of enhanced corrosion at the solution line requires discussion. The upper surface of an anode that had been oxidised for 60 days in an electrolyte containing 200 mg/L chloride is shown in Fig. 13. Evidence of solution line corrosion between the lower surface that is covered with a manganese dioxide scale and the upper original alloy surface is apparent. It appears that corrosion at the solution line is accompanied by or due to the absence of a manganese scale. This behaviour was obvious to a greater or lesser extent in all corroded anodes. In the case of the anodes operated with 400 mg/L in the electrolyte, this corrosion was so severe as to completely destroy the anode at the solution line.

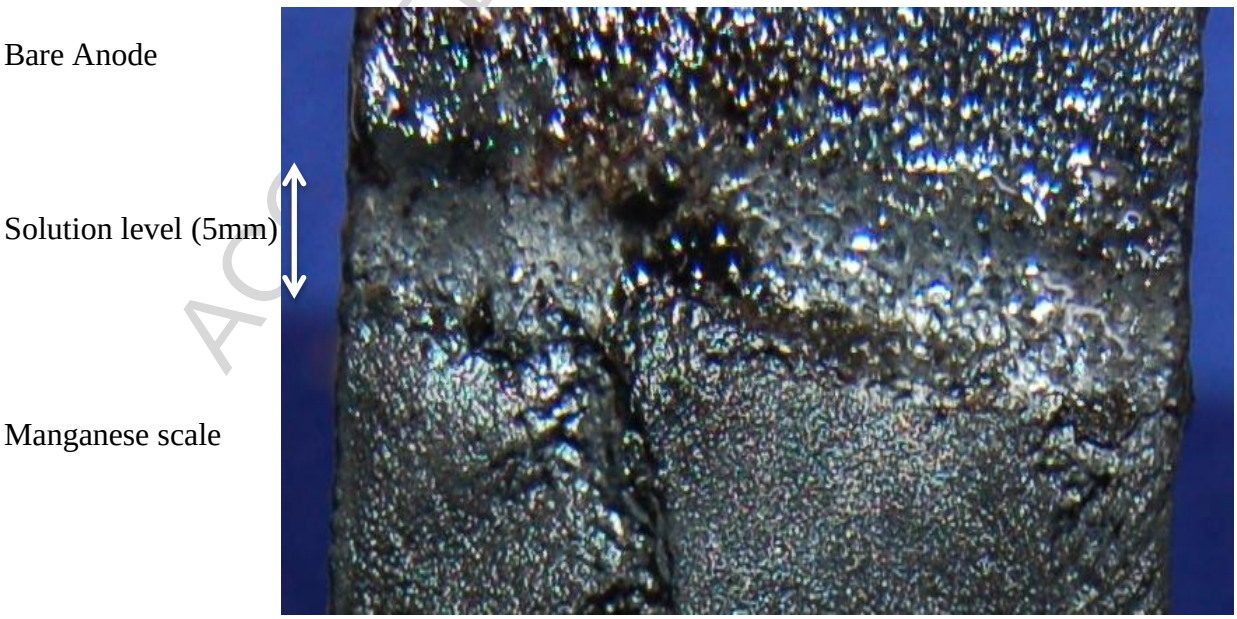

Fig. 13. Surface of an anode after 60 days operation in an electrolyte containing 200 mg/L chloride.

As a result of the breaking of oxygen bubbles close to the anode at the surface of the electrolyte, the solution line is continually moving vertically creating a thin electrolyte layer with concommitant higher IR drop to the cathode. This coupled with the presence of a meniscus that is present even in the absence of gas evolution, results in lower current densities in this area due to the higher impedance caused by the accumulated bubbles. It is suggested that at the resulting lower potentials, the rate of oxidation of manganese ions is reduced while that of chloride ions is largely unaffected. As a result, little or no manganese scale is formed although chlorine is evolved in the vicinity of the solution line. If, as has been suggested, corrosion of the alloy by chlorine is at least partially responsible for enhanced corrosion, then this mechanism is feasible.

In unpublished work, it was observed that localized corrosion under a layer of silicone sealant resulted in a five-fold local increase in anode corrosion. Furthermore, there was no evidence of manganese oxides in the anode scale in the corroded area although the main body of the anode was covered in a thick manganese-containing scale. It is possible that the high acidity and lower potential in this region due to the iR drop within the layer could be responsible for the absence of manganese oxides and therefore for enhanced corrosion.

A simplified expanded (not to scale) drawing of the structure of the anode under operating conditions is shown in Fig. 14.

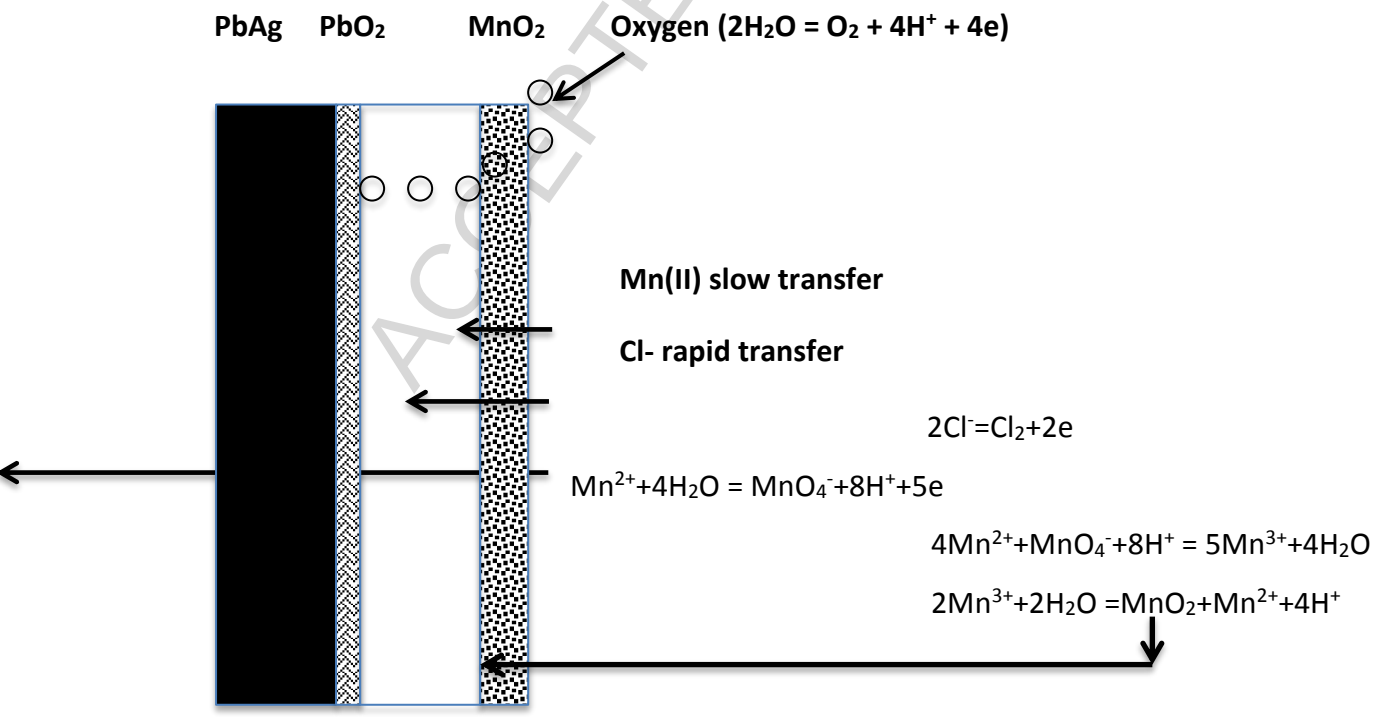

Electrolyte

Fig. 14. Expanded schematic of the anode structure and proposed reactions

It terms of this proposed structure, a relatively thin adherent layer of PbO_2 forms on the alloy surface by oxidation. The voluminous outer MnO_2 layer subsequently forms by chemical deposition with a thin layer of electrolyte below and within the pores of the MnO_2 (not shown). Oxygen evolution does not occur on the MnO_2 but on the PbO_2 surface and oxygen bubbles escape through cracks and fissures in the MnO_2 layer. As a result of the oxygen evolution reaction, the acidity in the interstitial electrolyte increases as shown in Table 8. It is assumed, without direct evidence, that tranfer of manganese ions through the MnO2 layer is hindered whereas that of chloride ions is not. Oxidation of manganese(II) to permanganate (and possibly also manganese(III)) and chloride to chlorine occurs in paralllel with oxygen evolution on the PbO_2 surface. Subsequent reaction of permanganate with manganese ions is slow due to the low manganese(II) concentration in the interstitial electrolyte (Table 8). However, this reaction does contribute to the formation of MnO_2 that slowly grows from the inside of the layer.

6 Conclusions

The experimental results obtained from a series of laboratory scale electrowinning tests conducted over 5 months to quantify the effects of halides (chloride, fluoride and bromide) on the performance and corrosion of lead-silver anodes can be summarized as follows:

1. The rate of corrosion of the anodes is strongly dependent on the concentration of chloride ions with significantly enhanced rates at 400 mg/L relative to 200 mg/L. This is consistent with plant observations.
2. The presence of manganese ions acts to reduce the deleterious effects of high chloride ion concentrations.
3. In presence of hydrogen peroxide in amounts sufficient to reduce manganic ions and to minimize formation of a manganese scale on the anode, the rate of corrosion is reduced even in presence of 600 mg/L Cl. The consumption of chloride is also reduced in the absence of manganese(III) ions in the bulk electrolyte.

4. Accelerated corrosion appears to be initiated at some point in the life of the anode and this initiation time varies from anode to anode. The severe corrosion observed in failed anodes appears to be localized and often close to the solution line.
5. The rate of oxidation of chloride and manganese ions increases substantially at the point of accelerated corrosion.
6. The presence of bromide and fluoride in the electrolyte does not appear to accelerate anode corrosion.

Although a definitive explanation for enhanced local corrosion at high chloride concentrations has not been advanced, the nature of the accelerated corrosion suggests that a crevice-like corrosion process similar to that observed in previous studies in the absence of chloride ions is responsible for localized massive corrosion. This has been attributed to the presence of high acidity and permanganate ions between the manganese oxide layer and the alloy surface. It is suggested that oxidation of chloride ions by permanganate occurs close to the alloy surface and that the chlorine is also responsible for chemical attack of the alloy. Such corrosion does not apparently occur if oxidation of manganese to permanganate is prevented by controlled addition of peroxide.

It is apparent from this study that there is no "silver bullet" that will eliminate the problem of excessive corrosion. While the above will add to our understanding, the results may well not solve the problem which is best solved in the short term by removing chloride from the plant electrolyte and controlling the manganese concentration to a suitably safe level with however, the consequent problems of excessive anode scale and cell mud formation.

ACKNOWLEDGEMENTS

The authors would like to acknowledge the financial and technical support of Teck Metals Ltd. Approval to publish the results is also appreciated.

7 References

Bennett, J.E. 1980. Electrodes for generation of hydrogen and oxygen from seawater. Int. J. Hydrogen Energy. 5: 401-408.

Gonzalez, J.A., et al., 1998. Redox control in the electrodeposition of metals. US Patent No. 5833830

Hierzyk, R., Krupkowa, D. and Lach E. 1969. From the studies on the behaviour of chloride ions in the zinc electrolysis process. (Translated title). Rudy I Metale Niezelazne, R14 nr 4.

Hine, F., Ogata, Y. and Yasuda, M. 1988. Proceedings of the International Symposium on Electrochemistry in Mineral and Metal Processing (II) (edited by P. E. Richardson and R. Woods), The Electrochemical Society, Pennington NJ. p 425.

Ibers, J.A. and Davidson, N. 1950. A spectrophotometric study of tripositive manganese in hydrochloric acid solution. J. Amer. Chem. Soc. 72: 4744-4748.

Ivanov, I., Stefanov, Y., Noncheva, Z., Petrova, M., Dobrev, Ts., Mirkova, L., Vermeersch, R. and Demarel, J-P. 2000. Insoluble anodes used in hydrometallurgy. Part 1. Corrosion resistance of lead and lead alloy anodes. Hydrometallurgy. 57: 109-124

Kelsall, G.H., Guerra, E., Li, G. and Bestetti, M. 2000. Effects of manganese(II) and chloride ions in zinc electrowinning reactors. Electrochem. Soc. Proc. Vol 2000-14.

Levanov, A.V., Kuskov, I.V., Antipenko, E.E and Lunin, V.V. 2006. The kinetics of the reaction between permanganate and chloride ions in acid solutions. Russian Journal of Physical Chemistry. 80: 726-731.

Liu K.J., H. Lester H. and Peterson N.C., 1996. Kinetics of the permanganate ion - chloride ion reaction. Inorg. Chem. 12: 2128-2132.

McGinnity, J and Nicol, M, 2008. The Effects of Periodic Open-Circuit on the Corrosion of Lead Alloy Anodes in Sulfuric Acid Electrolytes containing manganese, Hydrometallurgy 2008, Soc Mining, Metallurgy and Exploration, Littleton, Colorado, pp 592-599.

McGinnity, J. and Nicol, M.J. 2014. The role of silver in enhancing the electrochemical activity of lead and lead-silver alloy anodes. Hydrometallurgy, 144: 133-139.

Newnham, R.H. 1992. Corrosion rates of lead based anodes for zinc electrowinning at high current densities. J. Appl. Electrochem. 22: 116-124

Pakhomova, G.N. and Marenkova, L.M. 1966. Sov. J. Nonferrous Metals. 8: 41

Rosseinsky, D.R. and Nicol, M.J. 1965. Kinetics and mechanism of the formation of manganese(111) from manganese(11) and manganese(V11) in aqueous perchlorate solution. Trans. Faraday Soc. 61: 2718-2721

APPENDIX

Photographs of anodes from selected cells

Cell 1B – 129 days **Cell 2B 129 days**

Cell 3A – 78 days

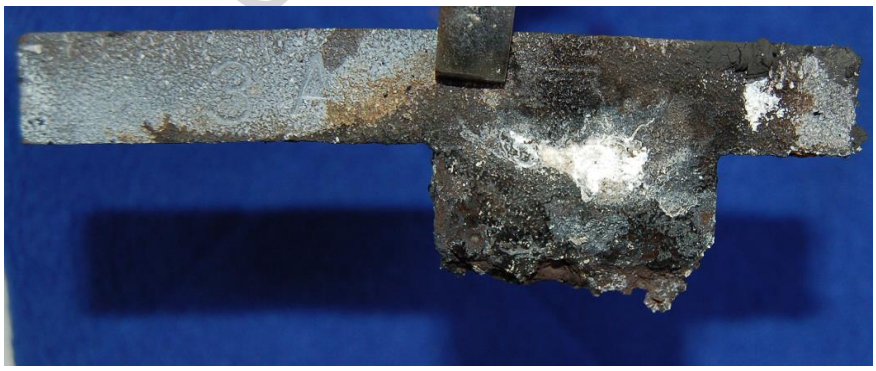

Cell 4A – 143 days

After cleaning

Cell 5A – 74 days

Cell 7A – 103 days

Cell 8B – 149 days
After cleaning

Cell 9A – 72 days

Cell 10B – 44 days

Cell 11A – 44 days

Cell 11A - After Cleaning

Highlights

- In the absence of manganese, oxidation of chloride does not occur on $PbSO_4$ but readily on PbO_2 .
- Oxidation of chloride occurs at the mass-transport controlled rate during the electrowinning of zinc in the absence of manganese.
- The rate of oxidation of chloride is significantly lower in the presence of manganese in the range 1 to 5 g/L.
- The use of periodic current reversal does not increase the rate of oxidation of chloride in the presence of manganese.
- The rate of anodic oxidation of chloride in the presence of manganese ions is too low to be of practical value in controlling chloride levels.